Beyond the Free Spectral Range: On-Chip Spectrometer with Multi-color Cascaded Colloidal Quantum-Dot Photodiodes

Chao Pang[1,2,3(✉)], Raúl López March[1], Ezat Kheradmand[2,3], Yu-Hao Deng[2,3], Luis Moreno Hagelsieb[4], Lukas Elsinger[1,2,3], David Cheyns[4], Pieter Geiregat[2,3], Zeger Hens[2,3], and Dries Van Thourhout[1,2]

[1] Photonics Research Group, Ghent University - imec, 9052 Gent, Belgium
Chao.Pang@Ugent.be
[2] NB Photonics, Ghent University, 9052 Gent, Belgium
[3] Physics and Chemistry of Nanostructures Group, Ghent University, 9000 Gent, Belgium
[4] IMEC, 3001 Leuven, Belgium

Abstract. Colloidal quantum dots (QDs), as a low-cost, flexibly tunable and fabrication scalable semiconductor material, have demonstrated exceptional capabilities in many complex applications including high-quality displays, high-resolution infrared imaging, advanced spectrometry and integration into photonic circuits. This study explores combining the tunable spectral response features of QD-based photodiodes (QDPDs) with dispersive photonic integrated circuits (PICs), demonstrating a spectrometer with operational spectral range extended beyond its original free spectral range (FSR). Experimentally, two types of PbS QDPDs, with different absorption features, were integrated in cascade on the output channels of a planar concave grating (PCG) with a 90 nm FSR. The differential responses of these QDPDs to two adjacent diffraction orders of the PCG enabled the creation of a spectrometer with a spectral range of approximately 180 nm, effectively decoupling two FSRs of the PCG. The proposed cascaded QDPDs, with diverse spectral photodetection capabilities, present great potential when integrated into complex optical systems.

Keywords: Photonic integrated circuits · colloidal quantum dots · spectrometer

1 Introduction

While complex devices such as arrayed waveguide grating (AWG) or planar concave gratings (PCG) are commonly used in silicon photonics as dispersive components [1–4] for on-chip spectrometers, a fundamental trade-off exists between their spectral range and spectral resolution [5]. Achieving better spectral resolution within a similar footprint requires larger optical dispersion, typically implying a larger diffraction order and, consequently, a smaller FSR and a narrower spectral range. This traditional trade-off persists because a single photodetector is used to detect light in each channel, making it challenging to distinguish optical signals from adjacent diffraction orders. If we place

J. Witzens et al. (Eds.): ECIO 2024, SPPHY 1069, pp. 1–6, 2024.
https://doi.org/10.1007/978-3-031-63378-2_28

multiple, different types of photodetectors on each channel in cascade, each with distinct responses to different diffraction orders, we are able to separate signals from more than one FSR, thereby eliminating the aforementioned trade-off. The flexibility in absorption tuning offered by QDs positions them as promising candidates for implementing this approach.

In this work, we propose and demonstrate the integration of the tunable features of QDs with dispersive PICs, pushing the spectral range beyond a single FSR. In our demonstration, we integrated two distinct types of QDs with excitonic absorption peaks centered around the wavelengths of two adjacent diffraction orders of the PCG. These QDs were integrated as waveguide-coupled photodiodes in cascade on the output channels of the PCG, each exhibiting a unique spectral response. By carefully designing the response of the QDPDs, we demonstrated a spectral range of approximately 180 nm using an eight-channel PCG with a FSR of 90 nm, breaking the FSR limit of the spectrometer.

2 Principle

In an optical dispersive component, such as a PCG, light with different wavelengths is deflected to distinct angles and collected by separate channels, as shown in Fig. 1(a). However, each channel contains light from different diffraction orders, separated by the FSR. In conventional dispersive spectrometers, a single photodetector is placed on each channel, converting optical power into an electrical signal for readout, as shown in Fig. 1(b). The presence of a single photodetector on each channel implies that optical signals from different diffraction orders are indistinguishable, limiting the working spectral range to one FSR.

Contrastingly, by incorporating multiple photodetectors with distinct wavelength responses for each channel, as shown in Fig. 1(c), different responsivities at various diffraction orders are achieved. This innovative approach provides additional information, enabling the separation of signals from different diffraction orders. In detail, considering an input signal with a power spectral density of $P_{in}(\lambda)$, the power density measured by the PCG is discretized into $P_{in}(\lambda_{i,k})$, where $\lambda_{i,k}$ is the peak transmission wavelength of channel i within diffraction order k. For two diffraction orders and two cascaded QDPDs at channel i, the power density at each order is linked to the photocurrents of these QDPDs by a 2×2 matrix $\boldsymbol{M_i}$:

$$\begin{bmatrix} I_{i,1} \\ I_{i,2} \end{bmatrix} = \begin{bmatrix} m_{i,11} & m_{i,12} \\ m_{i,21} & m_{i,22} \end{bmatrix} \begin{bmatrix} P_{in}(\lambda_{i,1}) \\ P_{in}(\lambda_{i,2}) \end{bmatrix} \tag{1}$$

Here, $I_{i,j}$ is the photocurrent measured by QDPD of type j at channel i. For any unknown input spectrum, we can retrieve it by measuring $I_{i,j}$ and solving this linear problem. The matrix elements $m_{i,jk}$ are determined by the channel responsivity $R_{i,j}(\lambda)$ of QDPD j around the peak transmission wavelength $\lambda_{i,k}$ of channel i, diffraction order k:

$$m_{i,jk} = \int_{\lambda_{i,k}-\frac{\Delta}{2}}^{\lambda_{i,k}+\frac{\Delta}{2}} R_{i,j}(\lambda) d\lambda \tag{2a}$$

$$R_{i,j}(\lambda) = R_{cas,j}(\lambda) T_{PCG_i}(\lambda) \tag{2b}$$

Here, $R_{cas,j}(\lambda)$ is the responsivity of the cascaded QDPD of type j (Fig. 1(c)), $T_{PCG_i}(\lambda)$ is the transmission spectrum of channel i of the PCG, Δ is the width of the channel spectral responsivity peak, as shown in Fig. 1(c). In practice, $R_{i,j}(\lambda)$ can be measured by sweeping a monochromatic light source and recording the photocurrent of each QDPD.

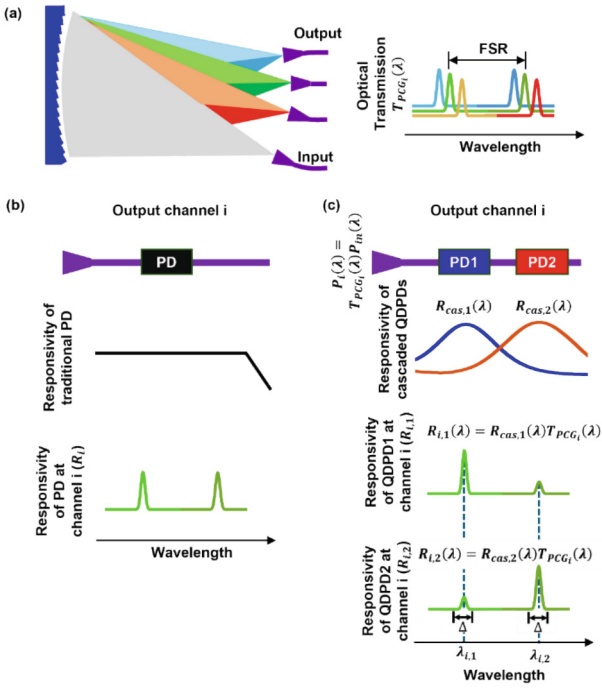

Fig. 1. Principle of breaking the FSR limit. (a) Planar concave grating and optical transmission at different channels. (b) Traditional photodetection solution for a spectrometer. Signals from different diffraction orders are mixed, so working range is limited to one FSR. (c) Cascaded QDPDs for photodetection. Different QDPDs have different response to different diffraction orders, extra information is achieved for separate signals beyond single FSR.

3 Experimental Results

The fabrication took place in the cleanroom facilities of Ghent University. Initially, the PCG, excluding the reflectors, was fabricated on a 300 nm SiN layer deposited atop 3 μm buried oxide substrates, utilizing E-beam lithography (EBL) and reactive ion etching (RIE) dry etching. Subsequently, another round of EBL and RIE was employed to define etched facets, serving as retroreflectors. A metal coating of 5 nm Ti/100 nm Au/5 nm Ti was then evaporated onto the facets, enhancing reflection and reducing insertion loss. The remaining metal on the chip was removed through lift-off techniques. The chip was then planarized with a 370 nm flowable oxide (hydrogen silsesquioxane,

HSQ) as a top cladding, providing a smooth interface for subsequent integration. This cladding also reduced optical power density in the QDPD integrated on top, mitigating power saturation and improving the linear response range.

Next, the QDPD stacks were integrated, starting from the planarized waveguide, as depicted in Fig. 2(a). Initially, a 20 nm thick indium tin oxide (ITO) layer was sputtered as the bottom electrode, followed by HCl-based wet etching to confine the ITO to the target QDPD regions as shown in Fig. 2(b). Subsequently, a 50 nm ZnO layer was deposited using sol-gel chemistry, patterned with dilute HCl solution, as shown in Fig. 2(c). We then place 20 nm Ti/100 nm Au n-contact pads on the side using the lift-off technique, as shown in Fig. 2(d). On top of the ZnO layer, we placed QD stacks for QDPD 1 and QDPD 2 using the lift-off method sequentially, as shown in Fig. 2(e) and (f). For QDPD 1, PbS QDs with a band-gap transition of 1250 nm were spin-coated as the absorption layer. This layer was treated with tetra-n-butylammonium iodide (TBAI) in a methanol solution to remove as-synthesized long surface ligands, turning the film n-type and enhancing the carrier mobility. On top, PbS QDs with a 940 nm band-gap transition were spin-coated and treated with ethanedithiol (EDT) in methanol solution for p-type doping. Layers of 1250 nm PbS-TBAI QDs and 940 nm PbS-EDT QDs were deposited, reaching a thickness of 60 nm each, and then lifted off simultaneously to achieve the desired pattern. QDPD 2 was processed similarly to QDPD 1, but with a 1355 nm transition bandgap for the absorption layer. Finally, 100 nm Au was placed on both types of QD stacks as p-contact pads. In the fabricated QDPDs, the ZnO/PbS-TBAI/PbS-EDT structure forms an n-i-p hetero-junction, aiding in carrier extraction and

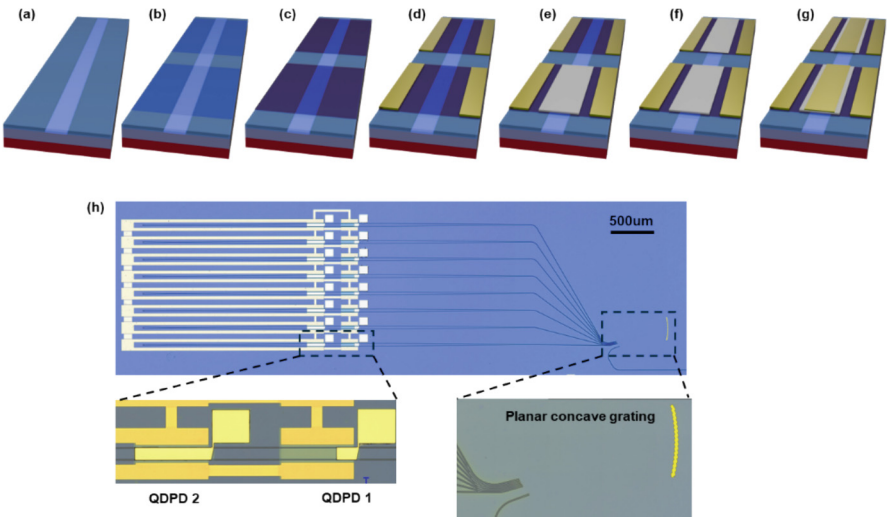

Fig. 2. Integration steps to fabricate cascaded QDPDs. (a) Optical passive structures fabrication and planarization. (b) ITO sputtering and patterning with wet etching. (c) ZnO deposition with solgel method and patterning with wet etching. (d) N-contact evaporation and pattering with liftoff. (e) Type 1 QDPD deposition and patterning with liftoff. (f) Type 2 QDPD deposition and patterning with liftoff. (g) P-contact evaporation and patterning with liftoff. (h) Top view of the fabricated spectrometer.

reducing dark current. The completed spectrometer, shown in Fig. 2 (h), features eight channels, each equipped with two cascaded QDPDs. All n-contacts were interconnected as a common ground to simplify measurements.

The wavelength dependent channel responsivity $R_{i,j}(\lambda)$ for both types of QDPDs was measured with a tunable laser, as shown in Fig. 3(a) and (b). As expected, QDPD 1 exhibits a stronger response to order 1, while QDPD 2 shows a more pronounced response to order 2. The capability of the spectrometer was demonstrated using amplified spontaneous emission (ASE) from an O-band semiconductor amplifier. Photocurrents were measured on both QDPDs at all eight channels for two different ASE spectra. With the 16 measured photocurrents and the transmission matrix M_i, input spectra were reconstructed, fitting well with those obtained from commercial benchtop spectrometers (Fig. 3(c)). Notably, both test spectra covered two FSRs of the PCG, making conventional spectrometers incapable of accurately reading the input spectrum.

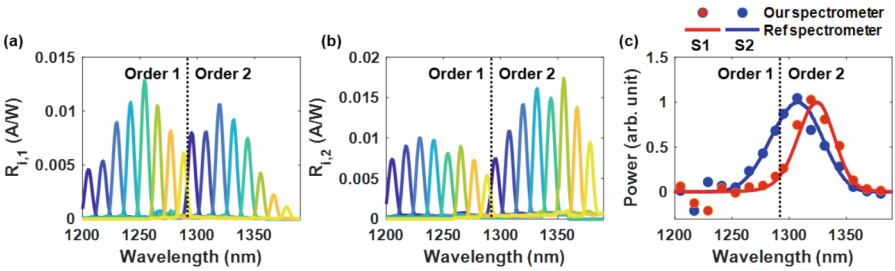

Fig. 3. Spectrum reconstruction. (a) and (b) Channel spectral responsivity of QDPD 1 and QDPD 2. (c) Reconstructed spectrum of spectrum S1 and S2 and their reference spectrum measured from a commercial spectrometer.

4 Conclusion

In this work, we have demonstrated an integrated spectrometer scheme using a PCG and cascaded QDPDs on a SiN platform. Leveraging the different wavelength response within the two consecutive QDPDs, we successfully decoupled two diffraction orders of the PCG. Our implementation achieved a broad operational range of approximately 180 nm on an eight-channel PCG with a 90 nm FSR, achieving a resolution of 12 nm. The tunable wavelength response of the proposed cascaded QDPDs opens avenues for their integration with various optical configurations, promising enhanced resolution, broader bandwidth, and increased robustness for on-chip computational spectroscopy applications.

References

1. Brouckaert, J., Bogaerts, W., Selvaraja, S., Dumon, P., Baets, R., Van Thourhout, D.: Planar concave grating demultiplexer with high reflective Bragg reflector facets. IEEE Photonics Technol. Lett. **20**, 309–311 (2008)
2. Brouckaert, J., Bogaerts, W., Dumon, P., Van Thourhout, D., Baets, R.: Planar concave grating demultiplexer fabricated on a nanophotonic silicon-on-insulator platform. J. Lightwave Technol. **25**, 1269–1275 (2007)
3. Pathak, S., Van Thourhout, D., Bogaerts, W.: Design trade-offs for silicon-on-insulator-based AWGs for (de)multiplexer applications. Opt. Lett. **38**, 2961 (2013)
4. Bogaerts, W., et al.: Silicon-on-insulator spectral filters fabricated with CMOS technology. IEEE J. Sel. Top. Quantum Electron. **16**, 33–44 (2010)
5. Kyotoku, B.B.C., Chen, L., Lipson, M.: Sub-Nm resolution cavity enhanced microspectrometer (2010)